



Growth and Spectral Characteristics of Grassland in Response to Different Soil Textures

Xiaochun Zhong^{1,2}, Junchan Wang³, Liu Tao⁴, Chengming Sun⁴,
Zhemin Li^{1,2}, and Shengping Liu^{1,2(✉)}

¹ Institute of Agriculture Information,
Chinese Academy of Agriculture Sciences, Beijing, China
{zhongxiaochun, lizhemin, liushengping}@caas. cn

² Key Laboratory of Agro-information Services Technology,
Ministry of Agriculture, Beijing, China

³ Lixiahe Regional Institute of Agricultural Sciences,
Yangzhou, Jiangsu Province, China
wjc@wheat. org. cn

⁴ Jiangsu Key Laboratory of Crop Genetics and Physiology,
Co-innovation Center for Modern Production Technology of Grain Crops,
Yangzhou University, Yangzhou, China
{tlIU, cmsun}@yzu. edu. cn

Abstract. Biomass and the chlorophyll content are important indicators to measure the growth and development of grasslands. Modeling using hyperspectral data is an important means to monitor grassland growth and development. In this paper, we studied Mexican maize grass, hybrid Pennisetum and hybrid Sudan grass under different soil texture treatments and determined the correlation between the canopy reflectance spectrum and plant growth status in different soil textures based on hyperspectral data. Our results showed that, under different soil texture treatments, the emergence rate of Mexican maize grass and hybrid Pennisetum did not differ significantly, whereas that of hybrid Sudan grass indicated a significant difference. Under different soil texture treatments, the trend of plant height variation was consistent. In terms of different types of grassland, it is generally feasible to establish a grassland yield spectral model based on the vegetation indexes NDVI and RVI, and the leaf SPAD values of the three types of grassland best fit the spectral parameter red edge area.

Keywords: Grassland · Biomass · SPAD value · Soil textures
Hyperspectral remote sensing

1 Introduction

Biomass is an important component of the ecosystem carbon pool, which is the main input source to the soil organic carbon pool [1]. Biomass is an important index to measure the growth and development of grassland and to guide production management [2]. Chlorophyll is an important pigment involved in grassland photosynthesis [3] and is

closely related to protein, nitrogen, moisture and other parameters [4]. It is a good indicator of photosynthetic efficiency and the development status of grasslands and also enables crop to exchange matter and energy with their surroundings. Therefore, the estimation of grassland biomass and the chlorophyll content has become an important method to evaluate grassland growth and development [5].

There are many grassland biomass and chlorophyll content acquisition methods; the traditional method has shortcomings such as being time and effort intensive, there are difficulties in scaling up, and vegetation is damaged [6]. Therefore, the traditional method cannot easily be used for the rapid acquisition of grassland biomass and chlorophyll content or the accurate monitoring of grassland growth and development. In recent years, with the application and development of hyperspectral remote sensing technology, hyperspectral data can be obtained by means of a hyperspectral imager, and quantitative analysis of weak spectral differences is carried out directly on the ground objects. The spectral diagnosis of plant leaf components is based on the spectral characteristics of plants. A large number of studies have shown a good correlation between the plant water, carbohydrate and chlorophyll contents and the spectral reflectance in specific bands [7]. Therefore, a relationship between the leaf components and the spectral reflectance can be established, and monitoring and diagnosis models of various plant biochemical parameters based on the reflectance spectrum can be developed; consequently, hyperspectral data have a strong advantage in grassland growth monitoring research [8].

Many domestic scholars have extensively studied the spectral characteristics of grasslands; the results show that grassland biomass and remote sensing vegetation indexes have a good correlation, but there are some differences in their correlation degrees [9]. In terms of a grassland biomass monitoring model, Clever et al. [10] studied a method to estimate grassland biomass based on a support vector machine that uses remote sensing data to extract grassland biomass and obtained the band with the best prediction ability. Chen et al. [11] studied the relationship between the grassland reflectance spectral characteristics of aboveground biomass, extracted a vegetation index from the spectral data, and established a dynamic monitoring model. In addition, the Dutch scholars Darvishzadeh et al. [12] used hyperspectral measurements of the grassland chlorophyll content. However, the grassland spectral characteristics may be limited by the environmental background, canopy structure, leaf moisture and soil texture.

In this paper, we studied the correlation between canopy reflectance characteristics and plant growth status under different soil texture treatments. We analyzed the sensitive bands and vegetation indexes that were closely related to plant biomass and nutrient status and established a plant biomass and SPAD value estimation model to promote the application of hyperspectral remote sensing technology in grassland growth and development monitoring and to provide a theoretical basis for large-scale, non-destructive and real-time monitoring of grassland growth using spectral technology.

2 Materials and Methods

2.1 Test Materials and Varieties

The experimental method is an indoor potting method. The experiment was conducted in 2016 at the Yangzhou University Agricultural College experimental farm. The tested varieties included three types of grasses: Mexican maize grass (A1), hybrid Pennisetum (A2), and South African hybrid Sudan grass (A3). Test pots: the plastic pot was 28 cm in diameter and 20 cm in height, and the bottom diameter was 18.5 cm. The surface area of the soil column was approximately 0.045 m^2 . Soil properties: test farm loam, of which the hydrolysable nitrogen was $149.2 \text{ mg}\cdot\text{kg}^{-1}$, the available phosphorus was $34.5 \text{ mg}\cdot\text{kg}^{-1}$, the available potassium was $84.6 \text{ mg}\cdot\text{kg}^{-1}$, and the soil organic matter content was 1.74%.

2.2 Experimental Design

According to the different soil textures, based on a quality ratio, three treatments, i.e., loam, loam:sand = 3:1, and loam:sand = 1:1, recorded as B1, B2 and B3, respectively, were established; each treatment consisted of 8 replicates. During the experimental period, the nutrient dosage was designed as N $120 \text{ kg}/\text{hm}^2$ ($0.54 \text{ g}/\text{pot}$), P₂O₅ $100 \text{ kg}/\text{hm}^2$ ($0.45 \text{ g}/\text{pot}$), K₂O $100 \text{ kg}/\text{hm}^2$ ($0.45 \text{ g}/\text{pot}$), applied once as basal fertilizer; the fertilizer and soil were well mixed and added to the pot.

Seed sowing: Mexican maize grass (A1) seeds: 10 seeds/pot; hybrid Pennisetum (A2) seeds: 100 seeds/pot; South African hybrid Sudan grass (A3) seeds: 60 seeds/pot. When sowing, some of the soil was removed from the pot; the remaining soil was compacted in the pot; the grass seeds were evenly spread on the soil surface; the removed soil was returned to the pot, compacted; and finally, spray irrigation was applied at low a low amount but quite frequently to ensure the top 3 cm of the soil surface remained moist during the seedling stage.

2.3 Measurements

2.3.1 Spectral Determination

After emergence, we sampled approximately once per month. At every sampling, two pots of each grass species per treatment were examined. When measuring the canopy spectrum, measurements need to be collected under sunny (not cloudy) conditions with good light. In addition, a single vegetation type with nearly 100% coverage should be selected to avoid interference from other vegetation and soil. Further, atmospheric water vapor absorption also affects the canopy spectral data, especially around 1400 nm and 1900 nm, where there is considerable noise. Therefore, the visible and near infrared bands are used to study the canopy characteristics of different herbs.

We used the United States ASD FieldSpec 3 Hi-Res field portable terrestrial spectrometer for spectral measurements. When measuring, the sensor probe was pointed down in a vertical direction, about 60 cm from the top of the canopy. Each replicate of each treatment was measured 9 times (i.e., measured 3 times right above the top of the test pot, then rotated about 120° and measured 3 times, and then rotated

about 120° and measured 3 times); the average value was taken as the spectral reflectance of that replicate, and finally the average value of 3 replicates was recorded as the spectral reflectance value of the treatment. Calibration of a standard blank was needed; therefore, calibration was performed after each treatment was measured.

2.3.2 Determination of the SPAD Value

We used a portable SPAD-502 chlorophyll meter in the test: 5 newly fully developed leaves per pot were selected, and we measured the SPAD value in the upper, middle and lower parts of each leaf and calculated the average.

2.3.3 Determination of Aboveground Biomass

We selected representative grass plants, cut the aboveground part at the roots, and determined the fresh weight of collected samples in the laboratory. Then, the samples were subjected to 105 °C for half an hour, followed by oven drying at 65 °C to a constant weight, after which the dry weight was determined as the aboveground biomass.

2.3.4 Determination of Soil Dry Density and Water Content

We measured the soil dry density and soil water content during the last two periods: we selected soil samples where the roots were concentrated in a pot; a ring knife was used to collect potted soil 5–10 cm from the surface; and the fresh weight was determined. Then, in the laboratory, the soil samples were dried in an oven at 80 °C to a constant weight; the dry weight was determined; and the soil dry density and water content were calculated.

2.4 Data Processing and Mapping

ASD viewspec-pro software was used to read the measured source spectral data, and the raw data were preprocessed and averaged as the spectral value of the process. Excel 2010 and SPSS16.0 were used for data processing and statistical analysis.

3 Results and Analysis

3.1 The Emergence Rate of Grass Species in Different Soil Textures

The seedling emergence rate is the proportion of emerged seedlings relative to the total seedlings that should emerge (%). As can be seen from Table 1, there was no significant difference in the emergence rate of Mexican maize grass (A1) and hybrid Pennisetum (A2) under different soil texture treatments. The emergence rate of hybrid Sudan grass (A3) under the B1 treatment was significantly higher than that under the B2 and B3 treatments.

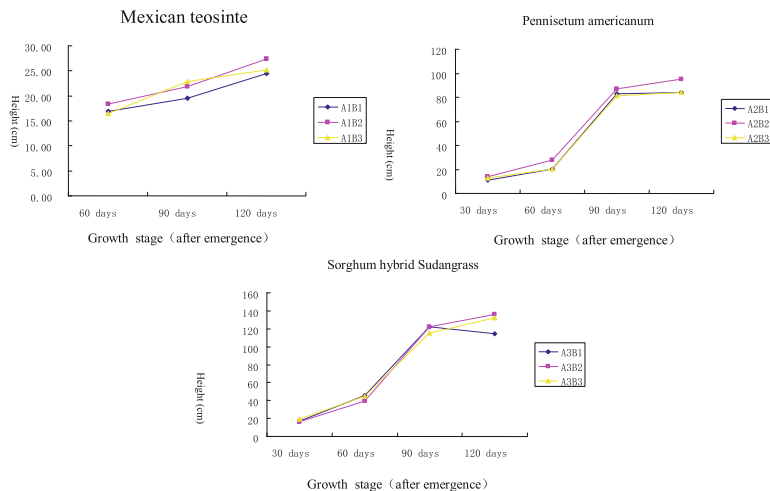
Table 1. The emergence rate of grass seed under different soil textures

Soil texture	Mexican teosinte A1	Pennisetum americanum A2	Sorghum hybrid sudangrass A3
B1	0.50a	0.41a	0.36a
B2	0.56a	0.49a	0.53b
B3	0.61a	0.51a	0.52b

The seedling emergence time was similar between hybrid Sudan grass and hybrid Pennisetum, whereas the emergence time of Mexican maize grass was later than that of the other two. However, the seedling emergence time was not significantly different between treatments for each species.

3.2 Plant Heights of the Grasses in Different Soil Textures and Periods

It can be seen from Fig. 1 that after emergence, the Mexican maize grass growth was relatively rapid, but then gradually slowed down. Hybrid Pennisetum was the fastest growing during the period from 60 to 90 days after emergence, and hybrid Sudan grass was the fastest growing during the period from 60 to 90 days after emergence.

**Fig. 1.** The plant height of grass under different soil textures and growth stages

3.3 Soil Dry Density and Water Content of the Grasses in Different Soil Textures and Periods

The soil dry density and water content of the test pots were measured by sampling test conducted 90 days and 120 days after emergence. The data in Tables 2 and 3 show a negative correlation between soil dry density and soil water content. This is because

across the three types of soil treatments, the sand content increased, soil dry density increased, and there was more sand and less clay; therefore, the soil permeability and ventilation capacity were good, but the water storage capacity was poor.

Table 2. The soil dry density (g/cm^3) of grass under different soil textures and growth stages

Soil texture	90 days after emergence			120 days after emergence		
	Mexican teosinte A1	Pennisetum americanum A2	Sorghum hybrid sudangrass A3	Mexican teosinte A1	Pennisetum americanum A2	Sorghum hybrid sudangrass A3
B1	1.07	1.08	1.21	1.11	1.06	1.08
B2	1.26	1.10	1.27	1.22	1.10	1.18
B3	1.42	1.36	1.35	1.30	1.31	1.21

Table 3. The soil moisture content (%) of grass under different soil textures and growth stages

Soil texture	90 days after emergence			120 days after emergence		
	Mexican teosinte A1	Pennisetum americanum A2	Sorghum hybrid sudangrass A3	Mexican teosinte A1	Pennisetum americanum A2	Sorghum hybrid sudangrass A3
B1	18.15	14.72	17.51	18.29	20.09	17.56
B2	14.33	8.53	13.49	13.88	11.96	13.33
B3	10.16	4.54	9.34	9.17	6.73	6.68

3.4 Dry Weight of Grasses in Different Soil Textures and Periods

It can be seen from Table 4 that the growth condition of Mexican maize grass under the B2 treatment was the best, but in the later stage of growth, the best growth occurred under the B3 treatment. The soil moisture content under the B3 treatment was more suitable for the late growth of Mexican maize grass.

Table 4. The dry weight (g/pot) under different soil textures and growth stages of Mexican teosinte

Soil texture	60 days after emergence	90 days after emergence	120 days after emergence
B1	18.70	38.05	50.85
B2	26.60	57.05	77.40
B3	19.70	49.10	86.80

It can be seen from Table 5 that there was no significant difference in the dry weight of hybrid Pennisetum in different soil textures, and the soil texture and water content had little effect on the growth of hybrid Pennisetum.

It can be seen from Table 6 that the growth condition of hybrid Sudan grass was the best in the middle and late growth stages under the B2 treatment, and the emergence rate was the highest under the B2 treatment. Thus, the soil with the B2 treatment was most conducive to the growth of hybrid Sudan grass.

Table 5. The dry weight (g/pot) under different soil textures and growth stages of *Pennisetum americanum*

Soil texture	30 days after emergence	60 days after emergence	90 days after emergence	120 days after emergence
B1	12.40	62.90	120.25	151.30
B2	16.80	68.40	124.80	147.10
B3	14.80	65.15	122.10	122.55

Table 6. The dry weight (g/pot) under different soil textures and growth stages of Sorghum hybrid sudangrass

Soil texture	30 days after emergence	60 days after emergence	90 days after emergence	120 days after emergence
B1	9.95	34.70	87.95	139.20
B2	7.85	45.75	104.50	153.85
B3	10.05	35.35	85.90	109.65

3.5 Relationship Between Dry Weight and Vegetation Index of Different Types of Grasses

We carried out correlation analysis of the dry weight and vegetation index of the grassland to test the degree of closeness between the two and to determine whether the sample can be used to determine the overall situation. The correlation coefficient is an important indicator to reflect this degree of closeness.

The correlation coefficients between four commonly used vegetation indexes, calculated using SPSS software, and the dry weights of different grasses are shown in Table 7.

Table 7. The correlation coefficient between vegetation index and dry weight of the three types of grass

Types		Vegetation index			
		NDVI	RVI	DVI	RDVI
Mexican teosinte	60 days after emergence	0.885*	0.937**	0.739	0.819*
	90 days after emergence	0.897*	0.894*	0.472	0.604
	120 days after emergence	0.921**	0.911*	0.36	0.529
Pennisetum americanum	30 days after emergence	0.910*	0.925**	0.459	0.683
	60 days after emergence	0.882*	0.910*	0.29	0.441
	90 days after emergence	0.941**	0.956**	0.209	0.48
	120 days after emergence	0.932**	0.904*	0.751	0.842*
Sorghum hybrid Sudangrass	30 days after emergence	0.877*	0.907*	0.746	0.816*
	60 days after emergence	0.943**	0.961**	0.56	0.692
	90 days after emergence	0.878*	0.912*	0.909*	0.916*
	120 days after emergence	0.893*	0.924**	0.14	0.592

It can be seen from Table 7 that there was a certain correlation between the normalized vegetation index (NDVI) and the ratio vegetation index (RVI) and grassland grass yield; therefore, it is feasible to establish a grass yield spectral model based on the two vegetation indexes. There were also some differences in the correlation between grass yield and different vegetation indexes, but there was no significant difference between the two vegetation indexes described above. Therefore, combined with the correlation between vegetation index and grass yield, different grassland types and fertility periods can be used in a practical and effective manner to establish a corresponding yield estimation model. Understanding the correlation between grass yield and vegetation indexes can help to further analyze the data, so as to achieve the purpose of determining the internal association within the data. After comparing various models, we found it best to use the power exponential model for estimation of grassland yield. Figures 2, 3 and 4 are analysis models of various types of grassland biomass and related vegetation indexes.

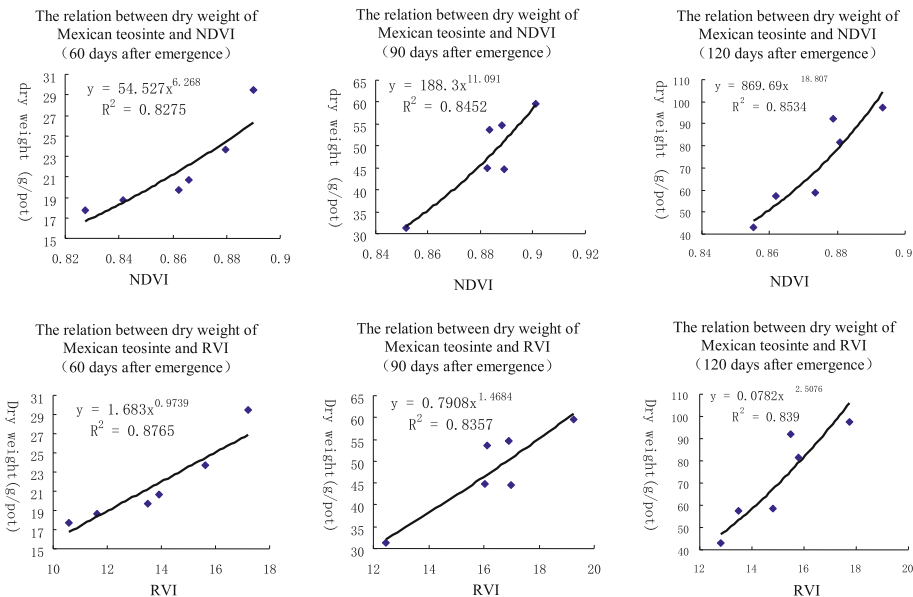


Fig. 2. The correlation between vegetation index (NDVI, RVI) and dry weight of Mexican teosinte under different growth

The corresponding yield estimation model and fitting effect of three types of grassland were different; the fitting effect is reflected by the R value: the greater the R value, the better the fit. The vegetation index was closely related to the dry weight of the grass, but the relationship between dry weights of the same type of grass and the two vegetation indexes (NDVI and RVI) was slightly different. There was also a difference between the vegetation index and the power exponential model of the dry weights of a particular grass at different growth stages.

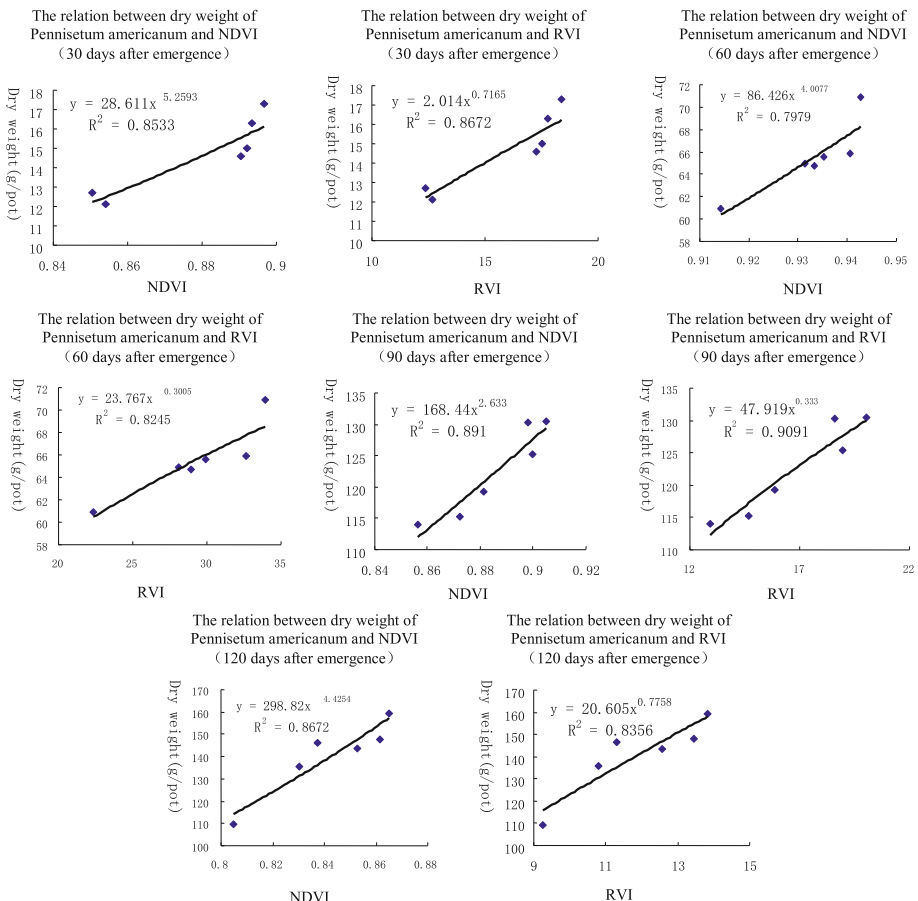


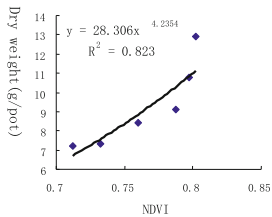
Fig. 3. The correlation between vegetation index (NDVI, RVI) and dry weight of *Pennisetum americanum* under different growth stages

Therefore, the grass yield model can be expressed as $y = ax^b$, where a and b are constants.

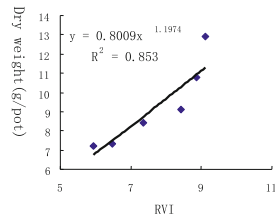
3.6 Relationship Between Dry Weight and Vegetation Index of Different Types of Grasses

Changes in the chlorophyll content will cause changes in plant leaf color. Under normal circumstances, the chlorophyll content can reflect the photosynthetic physiological state of plants to a certain extent. With an increase in the chlorophyll content, plant photosynthesis increases and is conducive to improving plant yield and quality [3]. Chlorophyll can describe crop canopy characteristics, reflecting leaf photosynthetic capacity and being used in the estimation of yield using the main parameters.

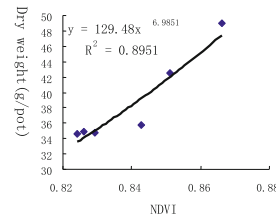
The relation between dry weight of Sorghum hybrid Sudangrass and NDVI (30 days after emergence)



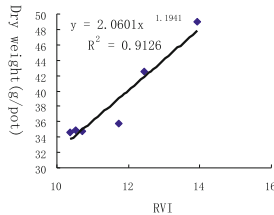
The relation between dry weight of Sorghum hybrid Sudangrass and RVI (30 days after emergence)



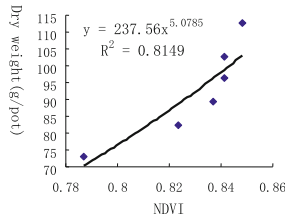
The relation between dry weight of Sorghum hybrid Sudangrass and NDVI (60 days after emergence)



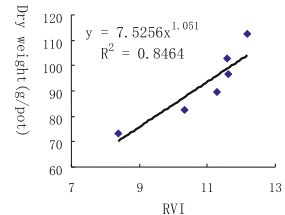
The relation between dry weight of Sorghum hybrid Sudangrass and RVI (60 days after emergence)



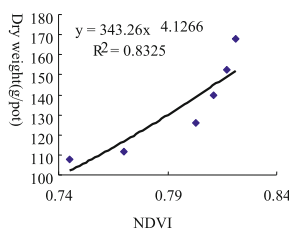
The relation between dry weight of Sorghum hybrid Sudangrass and NDVI (90 days after emergence)



The relation between dry weight of Sorghum hybrid Sudangrass and RVI (90 days after emergence)



The relation between dry weight of Sorghum hybrid Sudangrass and NDVI (120 days after emergence)



The relation between dry weight of Sorghum hybrid Sudangrass and RVI (120 days after emergence)

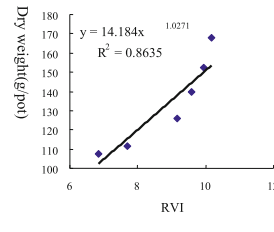


Fig. 4. The correlation between vegetation index (NDVI, RVI) and dry weight of Sorghum hybrid sudangrass under different growth stages

The information that chlorophyll conveys not only contains single leaf information but also part of the crop canopy information.

The phenomenon caused by the strong reflection formed by the absorption of vegetation chlorophyll in the red light band and the scattering of the near infrared band inside the leaf is called the red edge [4]. Previous studies have found close relationships between chlorophyll and red edge parameters.

The red edge parameters describing vegetation spectrum red edge characteristics in this paper mainly include [5, 6]:

- (1) Red edge position (λ_{red}): in the range of 680–750 nm; the corresponding wavelength of the reflection spectrum when the first order differential value reaches the maximum.
- (2) Red edge peak area: the area surrounded by the spectral first order differential value between 680–750 nm.

- (3) Minimum amplitude ($d\lambda_{min}$): the corresponding minimum first order differential value between 680–750 nm.
- (4) Red edge amplitude ($d\lambda_{red}$): the first order differential value when the wavelength is the red edge.
- (5) Ratio of red edge amplitude to the minimum amplitude $d\lambda_{red}/d\lambda_{min}$.

SPSS software was used to calculate the correlation coefficient between the SPAD value and the red edge parameter of entire growth period of different grasslands, as shown in Table 8.

Table 8. The correlation coefficient between the parameters of red edge and the SPAD value of the three types of grass

Types	Parameters of red edge				
	Red edge position λ_{red}	Red edge swing breadth $d\lambda_{red}$	Minimum swing breadth $d\lambda_{min}$	Ratio $d\lambda_{red}/d\lambda_{min}$	Peak area of red edge
Mexican teosinte	0.261	0.778**	0.654**	0.516*	0.747**
Pennisetum americanum	0.17	0.534**	-0.113	0.529**	0.603**
Sorghum hybrid sudangrass	0.454*	0.679**	0.524**	0.319	0.687**

It can be seen from Table 8 that the red edge area and red edge amplitude of the three grasses were significantly positively correlated with the SPAD values, and the red edge area was more strongly correlated with the SPAD values. We took the red edge area with the most relevant trait as the selected parameter and combined and established five estimation models based on the SPAD value of the red edge area: (1) Linear function model $y = a + bx$, (2) Logarithmic function model $y = a + b \times \ln(x)$, (3) Power function model $y = ax^b$, (4) Exponential function model $y = a \times e^{bx}$, and (5) Quadratic polynomial function model $y = ax^2 + bx + c$, to achieve the goal of a more accurate assessment of the SPAD value of grassland. The selection principle of the model is determined by the coefficient R^2 ; the larger the R^2 value, the better the model evaluation. According to the test results, among three grassland SPAD value estimation models, the quadratic polynomial model had the best estimation results.

Figure 5 results show that the SPAD value of the grassland was estimated practically and effectively by using the red edge area of the red edge parameter, and the SPAD value of hybrid Sudan grassland was the best among the three grassland types.

The reliability of the model was tested using the root mean square (RMSE), relative error (RE%) and determination coefficient (R^2). The results were plotted as a 1:1 correlation map to verify the optimal evaluation model of the grassland SPAD value.

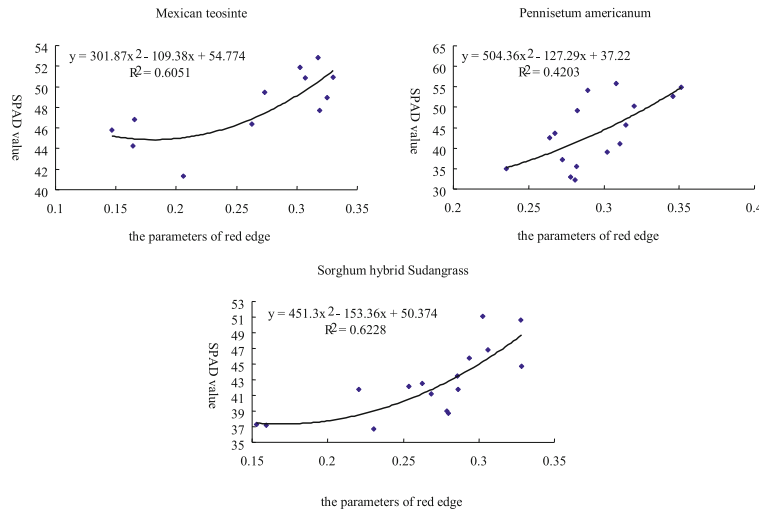


Fig. 5. The prediction models of SPAD value of the three types of grass

As shown in Fig. 6, the RMSE of the Mexican maize grass corresponding test model was 2.3218, the relative error RE was 3.53%, the determination coefficient R^2 was 0.7994, and the test accuracy was 96.47%.

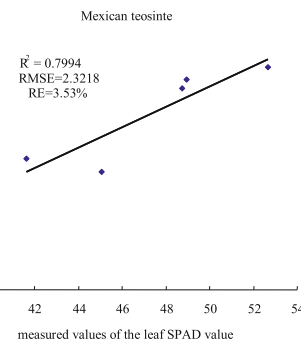


Fig. 6. The correlation between measured and simulated values of the leaf SPAD value of Mexican teosinte

As shown in Fig. 7, the RMSE of the hybrid Pennisetum corresponding model was 3.3678, the relative error RE was 6.99%, the determination coefficient R^2 was 0.655, and the test accuracy was 93.01%.

As shown in Fig. 8, the RMSE of the South African hybrid Sudan grass corresponding test model was 2.2721, the relative error RE was 4.50%, the determination coefficient R^2 was 0.8841, and the test accuracy was 95.50%.

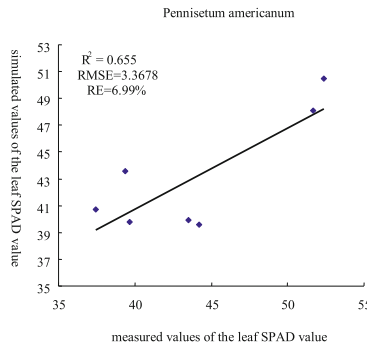


Fig. 7. The correlation between measured and simulated values of the leaf SPAD value of *Pennisetum americanum*

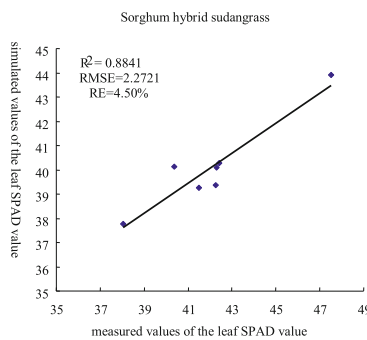


Fig. 8. The correlation between measured and simulated values of the leaf SPAD value of Sorghum hybrid sudangrass

4 Conclusion and Discussion

- (1) There was no significant difference in the emergence rate of hybrid *Pennisetum* and Mexican maize grass under different soil texture treatments. The hybrid Sudan grass had a higher emergence rate under the B2 and B3 treatments than the B1 treatment, and there was a significant difference.
- (2) There was no significant difference in plant height variation under different soil texture treatments. After emergence, the Mexican maize grass grew rapidly, and then the growth gradually slowed. The hybrid Sudan grass and hybrid *Pennisetum* grew the fastest during the period from 60 to 90 days after emergence.
- (3) The Mexican maize grass under the B2 treatment had the best growth condition in the early stage, but in the late growth stage, the soil water content under the B3 treatment was the most suitable. There was no significant difference in the dry weights of hybrid *Pennisetum* under different soil texture treatments during the entire growth period. It was observed that the soil texture and water content had little effect on the growth of hybrid *Pennisetum*. The hybrid Sudan grass under the B2 treatment had the best growth in the middle and late growth stage and the

highest rate of emergence; therefore, the soil texture in the B2 treatment was the most favorable for the growth of hybrid Sudan grass.

- (4) It is generally feasible to establish a yield estimation spectral model of different grasslands by using the vegetation indexes RVI and NDVI. The yield estimation model of grassland can be expressed as $y = ax^b$; a and b are constants.
- (5) We used the red edge peak area as the selected parameter, combined with the red edge peak area of the hyperspectral red edge parameter, and established a corresponding SPAD value estimation model; the quadratic polynomial model had the best estimation results. Among the three grassland types, the SPAD value estimation equation of Mexican maize grass was $y = 301.87x^2 - 109.38x + 54.774$; that of hybrid Sudan grass was $y = 451.3x^2 - 153.36x + 50.374$; and that of hybrid Pennisetum was $y = 504.36x^2 - 127.29x + 37.22$.

Acknowledgment. This research was supported by Technology Innovation Project Fund of Chinese Academy of Agricultural Sciences (2017).

References

1. Cao, M.K., Woodward, F.I.: Net primary and ecosystem production and carbon stocks of terrestrial ecosystems and their responses to climate change. *Glob. Change Biol.* **4**(2), 185–198 (1998)
2. Jmo, S., Johnson, K., Olson, R.J.: Estimating net primary productivity from grassland biomass dynamics measurements. *Glob. Change Biol.* **8**(8), 736–753 (2002)
3. Niinemets, U., Tenhunen, J.D.: A model separating leaf structural and physiological effects on carbon gain along light gradients for the shade-tolerant species *Acer saccharum*. *Plant Cell Environ.* **20**(7), 845–866 (1997)
4. Gáborčík, N.: Relationship between contents of chlorophyll (a + b) (SPAD values) and nitrogen of some temperate grasses. *Photosynthetica* **41**(2), 285–287 (2003)
5. Sun, J., Cao, H., Huang, Y.: Research advances of spectral technology in monitoring the growth and nutrition information of crop. *J. Agric. Sci. Technol.* **10**, 18–24 (2008)
6. Zhou, L., Xin, X., Li, G., et al.: Application progress on hyperspectral remote sensing in grassland monitoring. *Pratacultural Sci.* **26**(4), 20–27 (2009)
7. Qiao, X.: The Primary Investigation in Diagnosing Nutrition Information of Crop Based on Hyperspectral Remote Sensing Technology. Jilin University (2005)
8. Fan, Y., Wu, H., Jin, G.: Hyper spectral properties analysis of grassland types in Xinjiang. *Pratacultural Sci.* **23**(6), 15–18 (2006)
9. Zhichun, N., Shaoxiang, N.: Study on models for monitoring of grassland biomass around Qinghai lake assisted by remote sensing. *Acta Geogr. Sin.* **58**(5), 695–702 (2003)
10. Clevers, J.G.P.W., van der Heijden, G.W.A.M., Verzakov, S., et al.: Estimating grassland biomass using SVM band shaving of hyperspectral data. *Photogramm. Eng. Remote Sens.* **73**(10), 1141–1148 (2007)
11. Chen, J., Gu, S., Shen, M.G., et al.: Estimating aboveground biomass of grassland having a high canopy cover: an exploratory analysis of in situ hyperspectral data. *Int. J. Remote Sens.* **30**(24), 6497–6517 (2009)
12. Darvishzadeh, R., Skidmore, A., Schlerf, M., et al.: LAI and chlorophyll estimation for a heterogeneous grassland using hyperspectral measurements. *ISPRS J. Photogramm. Remote Sens.* **63**(4), 409–426 (2008)